IOPscience iopscience.iop.org

Home Search Collections Journals About Contact us My IOPscience

Epioptics: linear and non-linear optical spectroscopy of surfaces and interfaces

This article has been downloaded from IOPscience. Please scroll down to see the full text article.

1990 J. Phys.: Condens. Matter 2 7985

(http://iopscience.iop.org/0953-8984/2/40/001)

View the table of contents for this issue, or go to the journal homepage for more

Download details:
IP Address: 171.66.16.96
The article was downloaded on 10/05/2010 at 22:32

Please note that terms and conditions apply.

J. Phys.: Condens. Matter. 2 (1990) 7985–8006. Printed in the UK

REVIEW ARTICLE

Epioptics: linear and non-linear optical spectroscopy of surfaces and interfaces

J F McGilp
Department of Pure and Applied Physics, University of Dublin, Trinity College, Dublin 2, Ireland

Received 30 May 1990

Abstract. Recent developments in optical spectroscopy applied to surfaces and interfaces are discussed in this short review. It is shown that, by exploiting the underlying physics of the various techniques, submonolayer resolution can be obtained using photons as both probe and signal. Recent examples of the use of reflection difference spectroscopy, reflection anisotropy, spectroscopic ellipsometry, Raman spectroscopy and optical second-harmonic generation are described, with particular emphasis on ultra-high vacuum studies of systems which have been characterised using conventional surface probes.

1. Introduction

The study of condensed matter using optical techniques, where photons act as both probe and signal, has a long history, but it is only recently that the extraction of surface and interface information, with submonolayer resolution, has been shown to be possible. ('Optical' in this work applies to electromagnetic radiation in and around the visible region of the spectrum.) The large penetration depth of optical radiation into condensed matter makes the isolation of a surface or interface contribution difficult. The special efforts and techniques required to overcome this limitation of optical probes, together with the increasing activity in the area, justify distinguishing it from more conventional optical studies. The term 'epioptics' will be used (from the Greek 'epi-' meaning 'upon') (McGilp 1989).

The study of surfaces and interfaces using epioptic techniques offers several significant advantages over conventional surface spectroscopies (figure 1). The material damage and contamination associated with charged particle beams is eliminated; all pressure ranges are accessible; insulators can be studied without the problem of charging effects; buried interfaces are accessible owing to the large penetration depth of the optical radiation. In addition, epioptic probes offer micron lateral resolution and picosecond temporal resolution.

In this short review, recent examples of the use of reflection difference spectroscopy, reflection anisotropy, spectroscopic ellipsometry, Raman spectroscopy and second harmonic generation will be discussed, with particular emphasis being placed on ultra-high vacuum (UHV) studies of systems which have been characterised using conventional surface probes. A comprehensive review of the application of epioptic techniques to

0953-8984/90/407985 + 22 $03.50 © 1990 IOP Publishing Ltd

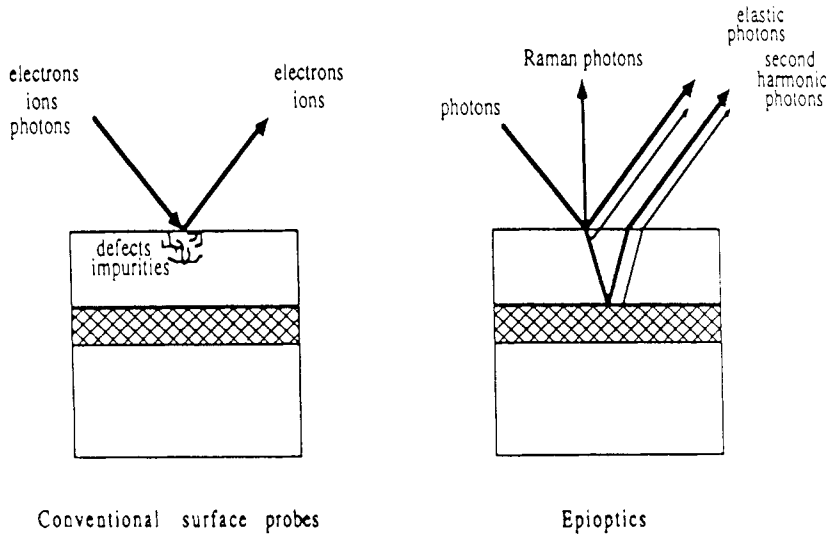

Figure 1. Comparison of conventional and epioptic probes.

organic thin films from the submonolayer to micrometre thickness range has appeared recently (Debe 1987).

2. Theory

2.1. General relations

The interaction of an electromagnetic (EM) field, of optical frequency ω and wave vector $\boldsymbol{k}$, with condensed matter is described in terms of a general polarisation amplitude, $\boldsymbol{P}(\boldsymbol{k}, \omega)$, induced by the field of amplitude $\boldsymbol{E}(\boldsymbol{k}, \omega)$:

$$\boldsymbol{P}(\boldsymbol{k}, \omega) = \varepsilon_0[\boldsymbol{\chi}^{(1)} \cdot \mathbf{E}(\boldsymbol{k}, \omega) + \boldsymbol{\chi}^{(2)} : \mathbf{E}^2(\boldsymbol{k}, \omega) + \boldsymbol{\chi}^{(3)} \vdots \mathbf{E}^3(\boldsymbol{k}, \omega) + \ldots] \tag{1}$$

where $\boldsymbol{\chi}^{(i)}$ is the ith-order dielectric susceptibility tensor describing the material response. In general, the susceptibility tensor will show both frequency and spatial dispersion (Hopf and Stegeman 1986). The more familiar dielectric tensor, $\boldsymbol{\varepsilon}$, is related to the susceptibility by

$$\boldsymbol{\varepsilon} = \varepsilon_0(\mathbf{1} + \boldsymbol{\chi}) \tag{2}$$

where $\mathbf{1}$ is the unit tensor.

In order to show the relationship between the various epioptic techniques discussed here, equation (1) is simplified and re-written (Geurts and Richter 1987),

$$\boldsymbol{P} = \varepsilon_0 \chi E(\omega) \tag{3}$$

where χ can be expanded in terms of the EM field, $E(\omega)$, a static field, $E(0)$, and some material deformation, Q,

$$\chi = \chi^{(1)} + \frac{\partial \chi^{(1)}}{\partial Q} Q + \frac{\partial^2 \chi^{(1)}}{\partial Q \, \partial E(0)} QE(0) + \chi^{(2)} E(\omega) + \ldots. \tag{4}$$

In equation (4) the first term describes reflection and ellipsometry, the second and

third terms describe inelastic Raman scattering where optical phonons are created and annihilated producing a frequency shift, and the fourth term, which produces a polarisation quadratric in the EM field, describes second harmonic generation and, more generally, three-wave mixing.

2.2. *Linear optical response*

Reflection and ellipsometry experiments measure changes which occur when EM radiation reflects from the interface between media. Standard texts on EM theory discuss this phenomenon in simple systems and general theoretical expressions for complex, multi-component systems have been derived (Heavens 1955, McIntyre and Aspnes 1971, Azzam and Bashara 1977). It is only relatively recently, however, that corrections to the classical model due to the variation of EM fields on the atomic scale in the interface region have been considered explicitly (Feibelman 1982). The linear optical response of surfaces has been reviewed recently (Olmstead 1987).

The underlying physics contained in reflection measurements can be seen by considering a simple two phase model where there is near-normal reflection from the surface of a homogeneous solid in vacuum (Debe 1987, Kleint and Merkel 1989). The reflection coefficient, $R(\omega)$, is measured as the ratio of the intensity of reflected to incident EM radiation. The amplitude of the reflected wave, r', is complex, with a real amplitude r and an imaginary part described by the phase, φ: $r' = r\exp(i\varphi)$ and $R = r'r'^*$ (complex quantities are primed). In ellipsometry measurements the ratio determined is that of r'_p/r'_s, the complex reflection amplitudes for p-polarised and s-polarised radiation, where p-polarisation has the electric field vector in the plane of incidence and s-polarisation has the vector perpendicular to this, in the plane of the interface. For a homogeneous solid the dielectric tensor (2) reduces to the scalar dielectric function, which is complex:

$$\varepsilon' = \varepsilon_1 + i\varepsilon_2. \tag{5}$$

The dielectric function is simply related to the complex refractive index, n':

$$\varepsilon' = n'^2 \qquad \text{where } n' = n + ik. \tag{6}$$

It follows that the two 'optical constants' of the solid, the real refractive index, n, and the extinction coefficient, k, are related to the dielectric function by

$$\varepsilon_1 = n^2 - k^2 \qquad \varepsilon_2 = 2nk. \tag{7}$$

The optical constants are linked to the measured reflection coefficient, R, and the phase, φ, by

$$n = (1 - R)/(1 - \sqrt{R}\cos\varphi + R) \qquad k = 2\sqrt{R}\sin\varphi(1 - 2\sqrt{R}\cos\varphi + R). \tag{8}$$

The phase is not directly measured, but must be determined from a Kramers–Kronig relation (Debe 1987, Kleint and Merkel 1989) after measuring R over a large frequency range:

$$\varphi(\omega) = \frac{\omega}{\pi}\mathcal{P}\int_0^\infty [\ln R(\omega')/(\omega^2 - \omega'^2)]\,d\omega' \tag{9}$$

where $\mathcal{P}$ denotes the Cauchy principal value. Equations (7)–(9) link the reflection coefficient to the dielectric function of the solid. It can be shown that ε_2 is related to the joint density of states which has singularities at critical points in the bulk band structure.

This leads to the well-known 'critical point analysis' of the reflectivity of solids (Wooten 1972).

Great care is required in ensuring that a sufficiently large frequency range is scanned before estimating the phase via Kramers–Kronig analyses (Debe 1987, Kleint and Merkel 1989). An error in measurement at one frequency produces errors at all frequencies for the calculated phase. Ellipsometry offers a significant advantage in this respect as measurements of phase with great sensitivity are possible. Ellipsometry provides direct access to the dielectric function which allows straightforward comparison with theory. A typical experimental approach (Aspnes and Studna 1983) measures tan ψ and cos Δ where

$$\rho' = r'_p/r'_s = (\tan \psi) \exp(i\Delta). \tag{10}$$

For EM radiation incident at an angle θ to the surface normal, the simple two phase model gives:

$$\varepsilon' = \sin^2\theta\{1 + \tan^2\theta[(1 - \rho')/(1 + \rho')]^2\}. \tag{11}$$

An important additional factor is that $r'_p = 0$ at the Brewster angle which depends on the refractive indices of the system: for more complex, absorbing systems r'_p is a minimum and there is a pseudo-Brewster angle (Azzam and Bashara 1977). Both r'_p and cos Δ are rapidly varying functions around the Brewster angle and maximum surface and interface sensitivity can be expected in this region.

The next level of complexity in the theory involves introducing a surface layer, of thickness d and dielectric function ε'_s, which may be either a heterogeneous thin film or simply the selvedge region of the solid where the electronic states differ appreciably from those of the bulk. This classical three phase model assumes a uniform dielectric function within the phase and a discontinuous change at the interface. Both the surface and bulk will now contribute to the reflectivity and so it is the change in reflectivity, ΔR, due to the presence of the surface layer, which must be measured. Where the thickness of the surface region, d, is much less than the wavelength of the EM radiation, λ, an approximation linear in (d/λ) can be used to derive an expression for this reflectivity change (McIntyre and Aspnes 1971). At normal incidence, for example,

$$(R(d) - R(0))/R(0) = \Delta R/R = (8\pi d/\lambda)\,\mathrm{Im}[(\varepsilon' - \varepsilon'_s)/(\varepsilon' - 1)] \tag{12}$$

where $R(d)$ is the reflectivity measured with the surface contribution, $R(0)$ is the reflectivity in the absence of the surface contribution, and ε' is now the bulk dielectric function. Equation (12) shows that optical absorption in the surface layer is necessary, together with a significant difference between surface and bulk dielectric functions, for ΔR to be measurable. It also shows that, at optical wavelengths, single atomic layers should, in principle, be detectable as reflectivity changes below 10^{-3} are readily measurable. A similar approximation can be used in ellipsometry to simplify the expression for the three phase complex reflection amplitudes (Azzam and Bashara 1977).

Equation (12) describes reflection difference spectroscopy (RDS), also referred to as the reflection difference (RD) method, surface reflectance spectroscopy (SRS), and differential reflectance (DR). The experiment compares measurements made with and without a contribution from the surface layer: the measurements require the surface to be changed and this can be a significant disadvantage. Where the surface layer is optically

anisotropic in the plane of the surface and the bulk is isotropic, an alternative, non-destructive approach is possible (Aspnes and Studna 1985, Aspnes 1985, Berkovits *et al* 1985). For orthogonal axes, x and y, in the surface plane, and normal incidence,

$$2(R_x - R_y)/(R_x + R_y) = (8\pi d/\lambda)\,\mathrm{Im}[(\varepsilon'_{xx} - \varepsilon'_{yy})/(\varepsilon' - 1)]. \tag{13}$$

The experiment is non-destructive as only azimuthal rotation of the sample or rotation of the optical plane of polarisation is required. The bulk response, being isotropic, gives a constant background. This technique has also been called RD and RDS, but will be referred to in this paper as reflection anisotropy (RA) (Del Sole 1990) to distinguish it from other forms of RDS. The above simple analysis shows that RDS, RA and spectroscopic ellipsometry are different experimental approaches to determining the surface dielectric function or, equivalently, the surface linear susceptibility.

The simple three phase model, upon which the above analysis is based, has been widely and successfully used, despite being fundamentally unphysical. Both the dielectric function and the normal component of the electric field are assumed to change discontinuously at the interface between phases, which requires an induced charge plane. 'Jellium' models of the response of an electron gas at an interface have provided some insight into the limitations of this three phase model (Feibelman 1982). The screening response differs between the surface and bulk because electron–hole pairs or plasmons may be excited at the surface, producing a short wavelength response from long wavelength external fields. The EM fields can no longer be assumed to be slowly varying on the scale of the selvedge and the response becomes non-local, with the field at one point in space affecting the fields at other points in space. The 'jellium' model indicates that the classical three phase model should work for s-polarised radiation, where the incident field is parallel to the surface, but the model is not valid for p-polarised radiation near and above the plasma frequency (Feibelman 1982). A more general model which includes the effects of crystallinity reaches similar conclusions (Del Sole 1981). Slab calculations of the linear optical response of semiconductor surfaces, using this more realistic formalism, have been reviewed recently (Del Sole 1990). A tight binding or pseudopotential calculation, with a slab of typically 12 to 18 atomic layers, is used to determine the slab dielectric tensor. This includes both bulk and surface transitions, but the bulk contribution is isotropic, allowing the identification of the surface contribution from the tensor anisotropy.

Turning briefly to Raman spectroscopy, the underlying theory of the scattering process is well understood both in classical and quantum terms (Long 1977). The main epioptic technique is phonon Raman scattering, although other single particle and collective excitations with smaller cross-sections can be important in two-dimensional electron gas systems (Geurts and Richter 1987). In outline, the incident radiation induces a dipole which will vary with some deformation coordinate, Q_1, representing the displacement of the ion cores of the system (equation 4). This deformation potential may produce elastic (Rayleigh) scattering, or inelastic (Raman) scattering where a phonon is created (Stokes process) or destroyed (antiStokes process). The Raman process is highly non-specular and has a small cross-section (typically one Raman photon per 10^{10} incident photons). It is only recently that instrumental advances have allowed Raman spectroscopy to demonstrate its potential as a surface and interface probe. It can be seen from equation (4) that the Raman effect is governed by third- and fourth-rank tensors. Crystal and molecular symmetry reduces the number of non-zero tensor components, giving rise to selection rules, while the magnitude of non-zero components can be determined from a perturbative approach (Long 1977, Debe 1987, Geurts and

Richter 1987). The Raman effect can be greatly enhanced by both local electric fields and electronic resonances at the excitation frequency, but this may involve a reduction in the amount of symmetry information available (Debe 1987). Raman spectroscopy thus provides vibrational information, in contrast to the other epioptic techniques discussed here which probe electronic structure, with the exception of sum frequency generation, discussed in the next section, which can also be used to provide vibrational information (Hunt *et al* 1987).

2.3. Non-linear response

Third-harmonic generation, in the absence of any strong resonantly enhanced surface electric dipole effects, is essentially a bulk probe, while higher order nonlinearities are too small to be significant. Second-harmonic generation and other three-wave mixing phenomena are potentially surface sensitive at non-destructive power densities. This is most easily seen for centrosymmetric materials where, in the standard multipole expansion of fields, the electric dipole term is parity forbidden, leaving only higher order contributions such as those from magnetic dipole and electric quadrupole effects. At a surface or interface the bulk symmetry is broken and electric dipole effects are allowed. An order of magnitude calculation shows that the surface effect should be comparable in size to the higher order bulk effects (Shen 1984, Guyot-Sionnest *et al* 1986). Cross-sections for three-wave mixing events are small, with typically one signal photon per 10^{13}–10^{16} incident photons.

Calculation of the surface nonlinear optical response is difficult, with the first frequency-dependent results from simple metal surfaces appearing recently (Liebsch 1988, Liebsch and Schaich 1989). For example, within a Green function approach, evaluation of $\chi^{(1)}$ involves a single Green function while $\chi^{(2)}$ involves a sum of products of two Green functions (Liebsch and Schaich 1989). The phenomenology, however, is well known and allows symmetry arguments to be used in the interpretation of experimental data (Guyot-Sionnest *et al* 1986, McGilp and Yeh 1986, Sipe *et al* 1987a, McGilp 1987a, b).

In the most general second order nonlinear response of a system, three-wave mixing occurs in which two incident fields of frequency ω_i and ω_j combine to produce a third field of frequency ω_k, where

$$\omega_k = \omega_i \pm \omega_j. \tag{14}$$

The four possible combinations and degeneracies in equation (14) can produce SHG, optical rectification, sum frequency and difference frequency generation (Hopf and Stegeman 1986). It is important to note that these processes are coherent and radiating fields have a well-defined direction; for example, SHG in the usual reflection geometry emerges along the path of the primary reflected beam, which simplifies detection.

The macroscopic theory of the bulk and surface SHG from cubic centrosymmetric crystals (Sipe *et al* 1987a) will be outlined here. Sum frequency generation expressions, where the two incident fields are different, will have lower symmetry, but little has been published in this area (Heinz 1982, Heinz *et al* 1989).

In the bulk of centrosymmetric crystals the lowest order non-linear polarisation density is of magnetic dipole and electric quadrupole symmetry. The effective polarisation can be written as

$$P_i(2\omega; \boldsymbol{r}) = \Gamma_{ijkl} E_j(\omega; \boldsymbol{r}) \nabla_k(\omega; \boldsymbol{r}) \tag{15}$$

where the gradient is determined with respect to the field coordinates and the summation convention is used (Sipe *et al* 1987a). For cubic crystals this expression reduces to

$$P_i(2\omega) = (\delta - \beta - 2\gamma)(\boldsymbol{E} \cdot \boldsymbol{\nabla})E_i + \beta E_i(\boldsymbol{\nabla} \cdot \boldsymbol{E}) + \gamma \nabla_i(\boldsymbol{E} \cdot \boldsymbol{E}) + \zeta E_i \nabla_i E_i \tag{16}$$

where δ, β, γ are isotropic constants and ζ is anisotropic (Bloembergen *et al* 1968). Only the last two terms contribute if excitation is by a single transverse plane wave.

Surface SHG can arise from higher order terms of this type, due to the large field gradients normal to the surface, and also from an electric dipole term because the inversion symmetry is now broken (Guyot-Sionnest *et al* 1986). These effects can be represented by an effective surface dipole polarisation density (Sipe *et al* 1987a),

$$P_i^s(2\omega) = \sum_{jk} \chi_{ijk}^s E_j E_k \delta(z - z_0^+) \tag{17}$$

where χ_{ijk}^s is the surface nonlinear susceptibility tensor which transforms with the point group symmetry of the surface. Expressions for the SH polarization can be obtained by applying boundary conditions (Heinz 1982) or by a more general Green function approach (Mizrahi and Sipe 1988). Sipe *et al* (1987a) have tabulated expressions for the total second harmonic fields from the (001), (110) and (111) faces of cubic centrosymmetric crystals.

Where surface and bulk contributions are of similar size it is difficult to distinguish the two contributions on the basis of symmetry arguments alone (Guyot-Sionnest *et al* 1986, Sipe *et al* 1987b) and this caused some controversy in earlier work (Guidotti *et al* 1983, Tom *et al* 1983, Litwin *et al* 1985). However, there are now many examples from metals and semiconductors where surface SHG has been clearly identified (Richmond *et al* 1988).

Appropriate choice of experimental geometry and polarisation vectors allows surface structural information to be deduced. For example, normal incidence experiments probe the in-plane anisotropy of the surface (Heinz *et al* 1985, Tom and Aumiller 1986) or the buried interface (McGilp and Yeh 1986, McGilp 1987a, b). For a solid with a surface or interface in the x–y plane, and normally incident radiation linearly polarised at an azimuthal angle φ to the x-axis, the SHG intensity is given by (McGilp and Yeh 1986, McGilp 1987a, b)

$$\begin{aligned} I_x(2\omega) &\propto |\chi_{xxx}^s \cos^2\varphi + \chi_{xyy}^s \sin^2\varphi + \chi_{xyx}^s \sin 2\varphi|^2 \\ I_y(2\omega) &\propto |\chi_{yxx}^s \cos^2\varphi + \chi_{yyy}^s \sin^2\varphi + \chi_{yxy}^s \sin 2\varphi|^2. \end{aligned} \tag{18}$$

The presence of symmetry elements in the surface simplifies these expressions; for example, components xyx, yyy, yxx are zero for $1m$ symmetry, while $mm2$ and $4mm$ symmetries have all components zero and no SHG in this geometry. Symmetry analysis is a powerful tool and it should be noted that the symmetry rules for the linear and nonlinear response are different.

3. Experiment

3.1. Linear optics

Linear optics experiments are appealingly simple in principle. Basic elements are a broad band lamp, polarising optics, monochromator and either a photomultiplier or

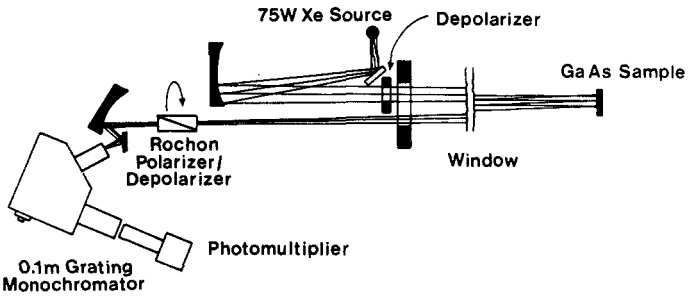

Figure 2. A rotating analyser RA instrument (after Aspnes *et al* 1988a).

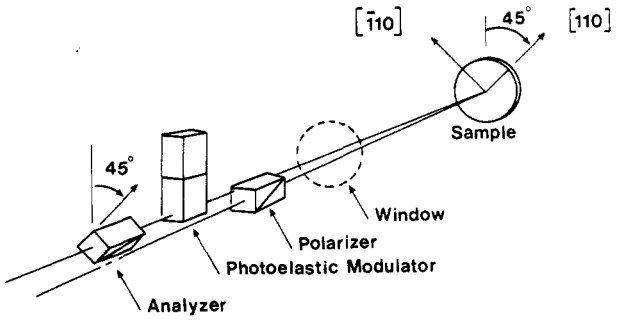

Figure 3. A photoelastic modulator version of the RA instrument, where the polariser replaces the depolariser of figure 2 and the modulator-fixed analyser combination replaces the rotating Rochon prism (after Aspnes *et al* 1988a).

semiconductor detector, depending on frequency. Difficulties arise because surface or interface effects in the optical response of unfavourable systems may be in the parts-per-million (ppm) range. It is in attempting to attain such high sensitivities that great care and ingenuity is required in experimental design.

In RDS experiments, the intensity variation which occurs with all broad band sources at these levels of sensitivity, together with the variation in detector gain, are major limiting factors which are dealt with in two basic ways: the optical path may be split between the sample and the detector (Gerhardt and Rubloff 1969, Huen *et al* 1971, Chiarotti *et al* 1971), or it may be split between the unknown sample and a reference sample (Chiaradia *et al* 1980, Blanchet *et al* 1981). Sensitivities in the 100 ppm range can be obtained using these techniques together with phase-sensitive detection and multiple reflection geometries.

The RA experiment is intrinsically easier, involving a single optical path and either sample or polarization rotation. Figures 2 and 3 show the simple configurations which may be used (Aspnes *et al* 1988a). In figure 2 a rotating analyser configuration is shown, while figure 3 shows how photoelastic modulation may be used instead. Sensitivities in the 10 ppm range, with a response time of 0.1 s, can be obtained with the latter technique due to the elimination of mechanical vibration (Aspnes *et al* 1988a).

Ellipsometry has a long history and many different types of instrument have been developed, although the majority are fixed wavelength systems (Azzam and Bashara

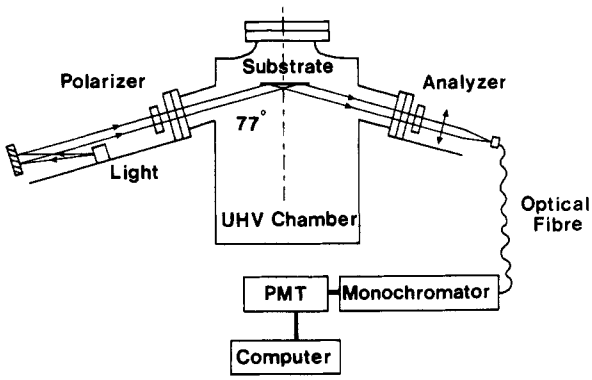

Figure 4. Schematic diagram of a spectroscopic ellipsometry system adapted for UHV studies (after Andrieu and Arnaud d'Avitaya 1989).

1977). Automated spectroscopic ellipsometry, using the rotating analyser technique and microcomputer control is a more recent development and is now a relatively mature technology with a number of commercial instruments becoming available, operating typically between 1.5 eV and 5 eV. A good instrument can determine ε' to 10 ppm (Aspnes and Studna 1975). The availability of microcomputers for both instrumental control and real-time analysis of results has produced a renaissance in ellipsometry. Figure 4 shows how a commercial instrument can be adapted for *in situ* UHV studies (Andrieu and Arnaud d'Avatiya 1989). As discussed in the theory section, maximum surface sensitivity is expected around the Brewster angle, which will be sample-dependent. Variable-angle spectroscopic ellipsometry (VASE) allows optimum choice of angle for a given system, but presents obvious window difficulties for *in situ* studies.

In situ measurements with all these techniques generally depend on the availability of suitable windows, although more complicated windowless constructions involving differential pumping stages have also been used (Kleint and Merkel 1989). Window design is critical if the full power of these epioptic probes is to be exploited. The window must have the widest possible spectral transmittance to enable accurate Kramers–Kronig transformations to be performed and to enable the dielectric function to be determined over a significant energy range. The other major requirement is minimal birefringence, as this limits polarization studies and, in particular, ellipsometry. This latter requirement limits the use of conventional wide transmittance window materials such as crystalline oxides and fluorides. Conventional glasses have been widely used but these suffer from a high energy cut-off at around 4 eV. UHV-compatible fused silica windows are now being fabricated which minimise birefringence problems and extend the cut-off to a much more useful 7.3 eV (Zandvliet and van Silfhout 1988, Andrieu and Arnaud d'Avitaya 1989, Studna *et al* 1989).

In contrast to the other linear optical techniques, a laser source is essential for Raman spectroscopy because of the small scattering cross-section (section 2). For detection, a double monochromator with a photomultiplier, or triple monochromation with an optical multichannel analyser, would typically be used (Debe 1987). Multiple monochromators reduce the scattered light to a minimum and allow the detection of the inelastic peaks which can lie within a few nanometers of the elastic peak. Raman photons backscattered from a surface or interface are distributed over 2π steradians,

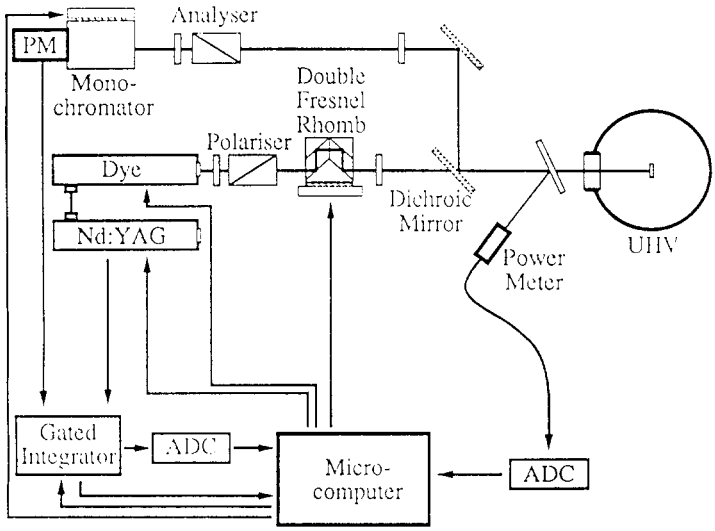

Figure 5. Apparatus for spectroscopic SHG studies of surfaces and interfaces under UHV conditions.

necessitating a small *f*/number collection lens: for UHV studies this will generally involve a re-entrant optical port. With optimal equipment the Raman spectrum of a molecular monolayer can be obtained in a few minutes (Debe 1987). Resonant Raman studies require, in addition, a tunable laser or a wide choice of discrete excitation wavelengths to allow access to a suitable electronic transition of the system. The polarization dependence of the Raman signal contains symmetry information and Porto's notation is commonly used to describe a particular experimental configuration (Damen *et al* 1966). For a scattering angle of 90°, the notation $i(jk)l$ represents an incident beam in direction i with polarization direction j, and a scattered beam in direction l with polarization direction k.

3.2. Non-linear optics

Pulsed lasers are the main excitation source for three-wave mixing experiments. Continuous-wave laser excitation of surface SHG has been reported (Boyd *et al* 1986), but surface damage considerations, together with the advantages of simple gating electronics, favour pulsed sources. A typical experiment would use nanosecond pulses of a few mJ energy, with a beam diameter of a few mm. Nd/YAG lasers have been widely used at 1064 nm excitation and, frequency-doubled, at 532 nm, while dye lasers are beginning to be used for wavelength-dependent studies. An experimental configuration allowing normal incidence studies is shown in figure 5. Where the SHG signal is very small the gated integrator can be replaced by a gated photon counter. Such systems have a remarkable discriminating power of 10^{18} between primary and second-harmonic photons.

4. Recent results

Epioptic studies, under UHV conditions, of systems characterised using conventional surface sensitive techniques will be highlighted here. There are recent reviews available

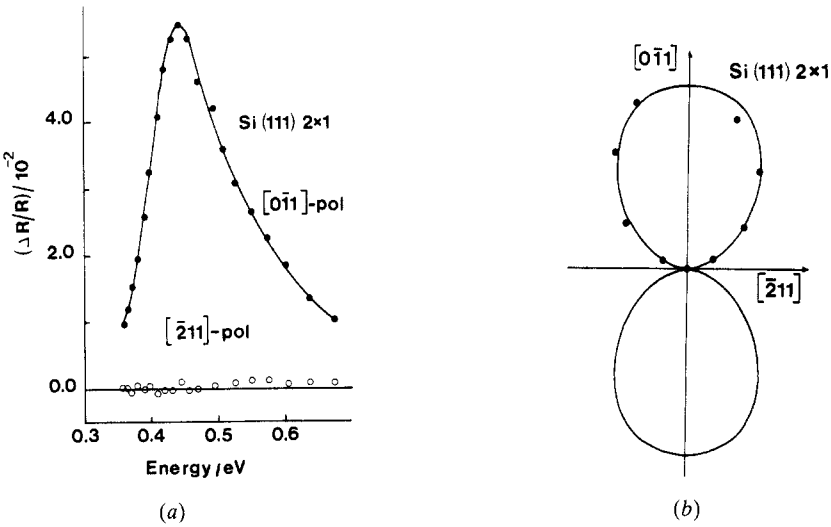

Figure 6. RDS of a Si(111) 2 × 1 single domain surface (*a*) $\Delta R/R$ as a function of energy and polarization; (*b*) polar plot of $\Delta R/R$ at the maximum: the solid curve is a $\cos^2$ fit to the data (after Chiaradia *et al* 1984).

on the linear optical properties of Si(111) and Ge(111) (Olmstead 1987), the theory of the linear optical spectroscopy of semiconductor surfaces (Del Sole 1990), Raman spectroscopy of adsorbates (Campion 1987), and SHG of interfacial structure and dynamics (Richmond *et al* 1988).

4.1. Linear optical response

4.1.1. Reflection difference spectroscopy. Recent work using RDS under UHV conditions has concentrated on semiconductor surfaces and, particularly, the (111) surfaces of Si and Ge (Olmstead 1987, Del Sole 1990). A result of major importance was obtained by Chiarotti, Chiaradia and co-workers after sustained effort over a number of years (Chiaradia *et al* 1984, Selci *et al* 1985). Polarisation-dependent RDS on single domain, cleaved, Si(111)2 × 1 revealed that the 0.45 eV surface state peak in the RDS signal was completely anisotropic (figure 6), giving a large signal when the polarisation was aligned parallel to the chains of the now generally accepted Pandey model of the surface (Pandey 1981, 1982). These results, when combined with the theoretical calculations of the optical response by Del Sole and co-workers (Del Sole and Selloni 1984, Del Sole 1990), allowed other contemporary models of the reconstructed surface to be ruled out. Similar results were obtained using photothermal displacement spectroscopy, where the thermal expansion of the sample, due to heating from surface optical absorption, is measured (Olmstead and Amer 1984).

Detailed comparisons of theory and experiment in the above-gap region are restricted in interpretation because the RDS experimental data conventionally compare clean and oxidised surfaces, while the calculations compare clean and hydrogen-terminated surfaces, the oxidised surfaces being ill-defined and computationally intractable (Del Sole 1990). RDS results from hydrogen-terminated surfaces would be of considerable theoretical interest. Above-gap experiments have been reported on Si(100) and Si(110)

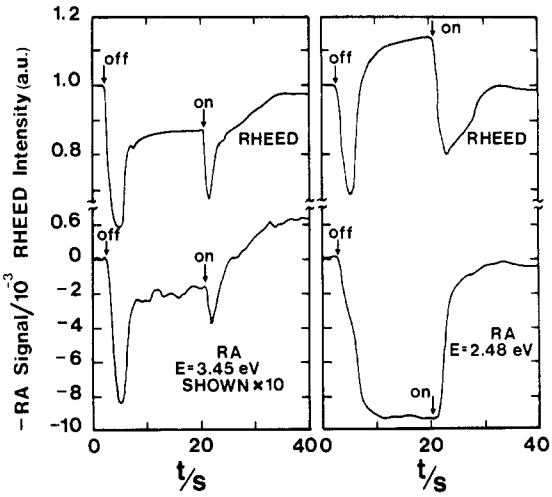

Figure 7. Simultaneously measured RA and RHEED for the As–Ga–As growth sequence on GaAs(100) at photon energies of (*a*) 3.54 eV, (*b*) 2.48 *eV* (*after Aspnes et al* 1988a).

surfaces (Wierenga *et al* 1979, 1980) and, recently, RDS of GaAs(110) and GaP(110) has been measured (Berkovits *et al* 1987, 1989, Selco *et al* 1987) and compared with theory (Manghi *et al* 1989). The lack of gap states with these latter surfaces leads to less spectacular results and underlies the need for more detailed and sophisticated calculations.

4.1.2. Reflection anistropy. As discussed in the theory section RA relies on the isotropic bulk response of cubic materials to allow the identification of the anisotropic surface response. Work has again concentrated on semiconductors and, in particular, III–V compounds, after initial work on above-gap anisotropies of native-oxide-covered Si(110) and Ge(110) surfaces by Aspnes and co-workers (Aspnes and Studna 1985, Aspnes 1985). Berkovits and co-workers (1985) made the first UHV studies on cleaved GaAs(110), and have recently studied (110) surfaces on InP, GaSb, InAs and InSb using both RA and RDS (Berkovits *et al* 1987). Results for GaAs(110) have been compared with theory (Manghi *et al* 1989) and also with the combination of direct and inverse photoemission measurements (Straub *et al* 1985), where reasonable agreement is found (Berkovits *et al* 1985). Further work in this area is anticipated.

These (110) surfaces would be expected to give a measurable RA signal due to their substantial structural ansitropy. A major breakthrough for RA came when molecular beam epitaxy (MBE) growth transients were observed on the GaAs(100) surface (Aspnes *et al* 1987, 1988a, b, c), The (100) surface is more isotropic than the (110) surface, but the RA signal, although smaller, is still detectable. It appears that the presence of group III element dimer bonds at the surface aligned along the [110] azimuth provides sufficient anistropy to obtain a measurable signal. Figure 7 shows simultaneously measured reflection high energy electron diffraction (RHEED) and RA transients for an As–Ga–As deposition sequence, for (a) 3.54 eV and (b) 2.48 eV photon energies. The former signal is clearly determined by the surface structure, while the latter, recorded at the maximum

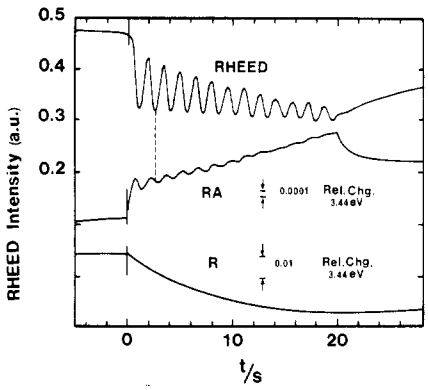

Figure 8. AlAs growth oscillations observed by RHEED and RA at 3.5 eV on the As-stabilized (2 × 4) AlAs surface (after Aspnes *et al* 1988c).

of the RA response, appears to be determined by the Ga–Ga dimer bond concentration and hence surface chemistry. Figure 8 shows RA oscillations during the growth of AlAs.

This work has recently been extended to organometallic vapour phase expitaxial (OMVPE) growth both at atmospheric pressure (Aspnes *et al* 1988d, 1989) and in a low pressure reactor under optimal growth conditions (Acher *et al* 1990). The RA signal is stronger than that obtained under MBE conditions, indicating that different surface species are involved. The kinetic behaviour agrees with an excluded-volume chemisorption mechanism for monolayer OMVPE growth at these pressures (Aspnes *et al* 1988d, 1989) and shows the potential of such epioptic probes for atmospheric studies of nucleation and growth.

A further significant development comes from the addition of sample rotation to the photoelastic modulation described in section 3 (Aspnes *et al* 1990). This second modulation of the signal reduces previously limiting systematic errors and allows the accurate determination of both the phase and amplitude of the complex reflection difference along the principal axes. The new ellipsometric nature of these data enables the anisotropy of the surface dielectric function to be determined directly. The results obtained for GaAs(100) under MBE growth conditions show structure at 1.8 eV, 2.6 eV and 4.1 eV, and comparison with a tight binding calculation identifies the first structure with a Ga dimer to Ga lone pair transition, the second with an As lone pair to As dimer antibonding state transition, and the third with an As dimer bonding to antibonding state transition (Aspnes *et al* 1990). The resonable agreement between experiment and a relatively simple calculation makes the application of this technique to other, less well understood, systems an exciting prospect.

4.1.3. Ellipsometry. The previous paragraph described the development of a new type of ellipsometry. In this section results using conventional ellipsometric techniques are discussed. Ellipsometry is widely used for studies of thin films in the ambient, where parameters such as film thickness, composition, and interface roughness are determined, but rarely with monolayer resolution (Gijzeman and van Silfhout 1983, Crean *et al* 1990). An exception to this is the increasing use of ellipsometry to determine layer number in Langmuir–Blodgett films (Debe 1987), while another area of current interest is the use

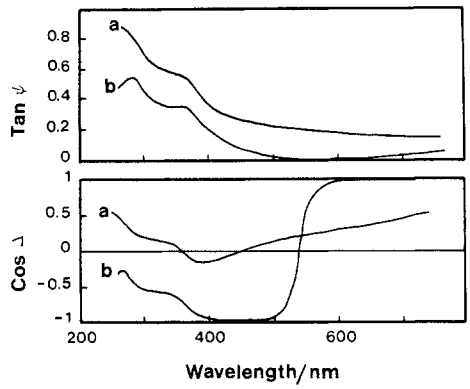

Figure 9. Variation of the ellipsometric parameters with wavelength for Si(111) (*a*) with 15 nm of oxide, (*b*) for the clean surface, at an incidence angle of 76°. Note the rapid variation in cos Δ around 530 nm, where the Brewster angle condition is satisfied (after Andrieu and Arnaud d'Avitaya 1989).

of spectroscopic ellipsometry to determine the effective dielectric functions of quantum well and superlattice structures (Freeouf *et al* 1990).

Early UHV studies were made by Bootsma's group on metals and small molecule adsorption (Habraken *et al* 1980). An example of monolayer (ML) sensitivity using ellipsometry is nicely illustrated by work on benzene physisorption on single crystal graphite between 180 K and 290 K, where the maximum optical thickness is consistent with one ML of molecules lying flat on the surface (Koort *et al* 1987). Recent work on semiconductors includes the identification of surface states on Ge(111) c2 × 8 and the effects of O_2 adsorption on Ge(001) 2 × 1 (Zandvliet and van Silfhout 1988, 1989) A good example of the sensitivity of spectroscopic ellipsometry is shown by the absorption of Sb_4 on Si(111), which has been followed in real time with a detection limit of 0.05 ML (Andrieu and Arnaud d'Avitaya 1989). This sensitivity has been obtained by working at the Brewster angle for the system. Figure 9 shows the variation of the ellipsometric parameters tan ψ and cos Δ with wavelength for (a) Si(111) with a 15 nm oxide layer (b) clean Si(111), for an incident angle of 76°. At around 530 nm this angle satisfies the Brewster condition, producing a dramatic change in cos Δ. Maximum surface sensitivity is obtained by working in this region, as discussed in section 3.

4.1.4. Raman spectroscopy. As discussed in section 2, Raman spectroscopy provides information on vibrational bands, in contrast to the other epioptic techniques reviewed which provide mainly electronic structure information. Some recent examples of UHV work in well-characterised single crystal surfaces and interfaces will be discussed here, but examples of surface enhanced Raman spectroscopy (SERS) will not be included because the technique relies on rough, and thus ill-characterised, surfaces to increase the local field (Debe 1987).

The majority of UHV studies have been of small molecule adsorption on metal surfaces (Campion 1987). The Raman vibrational bands of the free molecule shift and change in intensity on adsorption, and new bands may appear due to the reduced symmetry of the adsorbate–surface system. Selection rules have been determined for

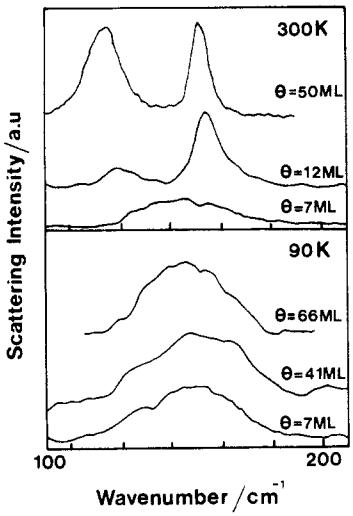

Figure 10. Raman spectra of Sb on GaAs(110) at 90 K and 300 K. The broad structures are from amorphous Sb and the peaks in the 300 K spectra are from rhombohedral crystalline Sb. The scattering configuration is $110(1\bar{1}0, 1\bar{1}0)\bar{1}10$ (see section 3) (after Geurts and Richter 1987).

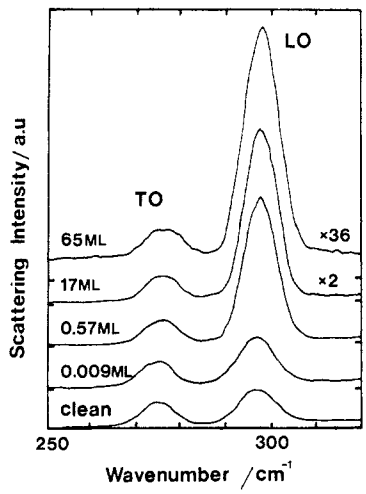

Figure 11. Raman spectra, using the same scattering configuration, of the substrate, GaAs(110), with increasing Sb coverage. The TO phonon originates from the usual deformation potential scattering, while the LO phonon comes from electric field induced scattering (after Geurts and Richter 1987).

both homogeneous and structured metal surfaces, where the presence of specific adsorption sites may lower the symmetry of the system. A good example of this effect is seen in a study of benzene, pyrazine and s-triazine adsoprtion on Ag(111) and Ag(110), where the different spectra obtained from the six possible combinations allowed the determination of the likely adsorption site geometry (Hallmark and Campion 1986). Further examples may be found in recent reviews (Campion 1987, Debe 1987).

The other area of UHV work has concerned semiconductor surfaces and interfaces. Submonolayer sensitivity to adsorbates has proved difficult to achieve, even with resonant Raman studies. At higher coverages the technique has been shown to have great diagnostic power. An example is the adsorption of Sb on GaAs(110) and InP(110), where the Raman signal from Sb becomes observable at 0.6 ML (Hünermann *et al* 1987, Pletschen *et al* 1986, Zahn *et al* 1986). A broad Sb signal reveals that the overlayer is amorphous up to 66 ML at substrate temperatures of 90 K, but that at 300 K crystallisation of the overlayer occurs around a coverage of 12 ML (figure 10). Comparison of peak positions and linewidths with those of bulk Sb reveal considerable strain in the film and an estimated crystallite size below 10 nm at lower coverage (Geurts and Richter 1987). The crystallites have their *c* axes normal to the substrate surface (Hunermann *et al* 1987).

Submonolayer sensitivity is, however, easily obtained in an important area of semiconductor interface studies. This relates to band bending at the surface and interface, which has direct relevance to electronic device design and performance. Resonant Raman spectroscopy is used, with the exciting radiation close to a bulk optical gap, generally the E_1 or $E_1 + \Delta_1$ gaps. Important results have been obtained using the Frölich interaction (the third term of equation (4), section 2), where the contribution to the Raman process from the substrate longitudinal optical (LO) phonon becomes allowed

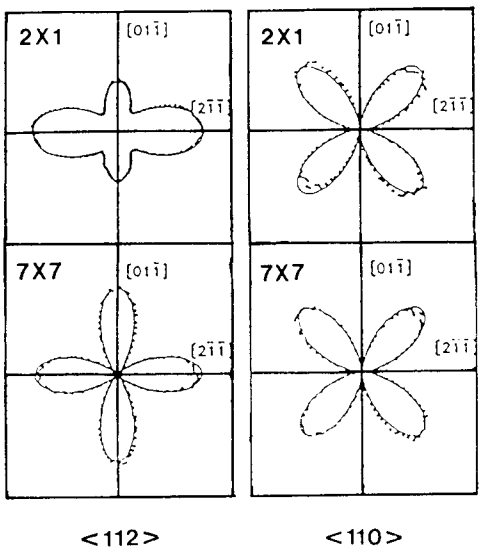

Figure 12. SHG intensity, polarised along the ⟨112⟩ and ⟨110⟩ azimuths, from Si(111) 2 × 1 and Si(111) 7 × 7 surfaces, as a function of the polarization of the normally incident pump beam (after Heinz *et al* 1985).

when the symmetry at the interface is reduced by the static electric field associated with band bending (Pinczuk and Burstein 1968). Oxide layers, heterostructures and metal–semiconductor interfaces have been studied (Geurts and Richter 1987). Figure 11 shows the transverse optical (TO) phonon and LO phonon signals from the GaAs(110) substrate as the Sb coverage increases. The LO/TO intensity ratio provides a measure of the band bending at the interface, for coverages of 0.01 ML to 65 ML (Pletschen *et al* 1986). Band bending at the buried interface shows strong variations above 10 ML which can be neatly correlated with the change in structure of the Sb overlayer revealed by the Sb Raman signals discussed above. This study shows the great potential of epioptic probes in linking surface and interface physics at low coverages with semiconductor device physics at high coverages.

4.2. Non-linear optical response

It was mainly the work of Shen's group in the early 1980s which established the potential of SHG as a surface and interface probe (Shen 1984, 1985). Important contributions also came from Sipe's group (Litwin *et al* 1985). The first UHV study, where conventional surface probes were used for characterization, appeared in 1984 and showed that adsorption of O_2 and CO damped the SH signal from the Rh(111) surface, while adsorption of Na enhanced it (Tom *et al* 1984). The last few years have seen a substantial increase in the number of UHV-based SHG studies and a selection of recent work is presented here.

As discussed in the theory section, azimuthal studies of rotational anisotropy at or near normal incidence can be used to probe in-plane symmetry. Interesting results have been obtained from (111) surfaces. The SH signal from Si(111) 2 × 1 and Si(111) 7 × 7 surfaces is shown in figure 12 and is clearly sensitive to the symmetry change between the two reconstructions, the solid lines being fits to equations (18) (Heinz *et al* 1985). The Au–Si(111) system (figure 13) was used to show that SHG can provide information about the in-plane symmetry of buried metal-semiconductor interfaces (McGilp and Yeh 1986, McGilp 1987a, b). By comparing results from Si(111) and Si(100) surfaces, and by monitoring the effects of exposure to background gases in the UHV system, it was

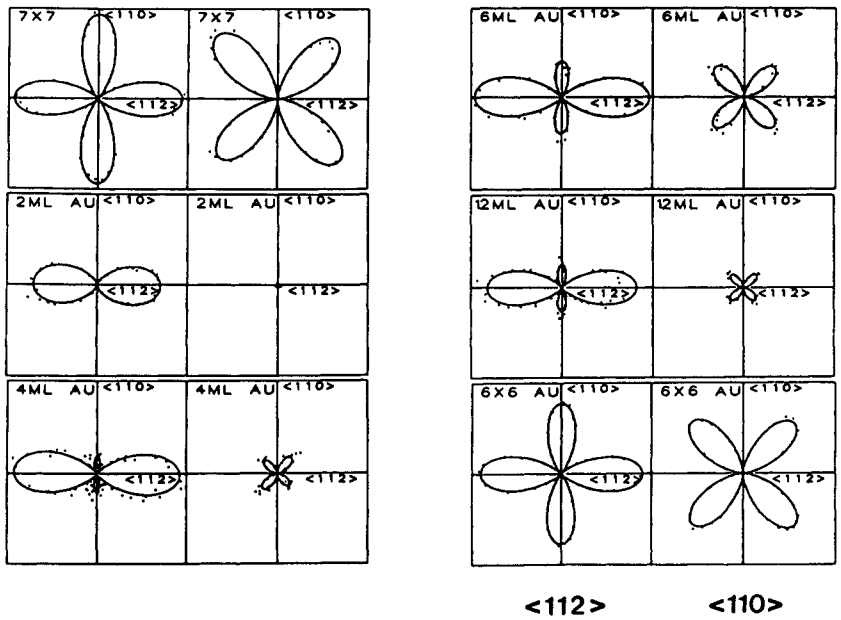

Figure 13. SHG intensity, polarized along the ⟨112⟩ and ⟨110⟩ azimuths, from Si(111) 7 × 7 and Si(111)–Au (after McGilp 1987a).

shown that the varying paterns of figure 13 were due to structural changes at the buried interface. The importance of the spectroscopic dimension was also stressed (McGilp 1987a), and angle-resolved photoemission and inverse photoemission data were used to show that there were interface states in the bulk band gap at the correct energies for enhancement of the SHG signal. Recent work on Si and Ge deposition on Si(100) has shown that the SHG response is also very sensitive to the electronic structure of the (100) surface (Hollering *et al* 1990).

Crystalline metal surfaces also show rotational anisotropy. The SH signal from the Cu(111) surface has a well-developed 3 m symmetry which is attributed to interband transitions involving d-electrons, as the free electron SH response is zero in this geometry (Tom and Aumiller 1986). The adsorption of H_2 on Ni(111) has been used to probe the sensitivity of SH signal to long range order. The order–disorder transition of the β_2 state of adsorbed hydrogen was monitored using low energy electron diffraction and SHG. No significant change in the SHG was observed and it was concluded that SHG only probes local site symmetry in this system (Anderson and Hamilton 1988). Whether the sensitivity of surface and interface SHG to long range order is system-dependent remains an open question.

Turning now to off-normal studies, Plummer's group has been investigating the SH response of clean and adsorbate-covered metal surfaces. They have shown that dynamical screening at a metal surface can be directly probed by SHG (Song *et al* 1988). Figure 14(*a*) shows the variation in SHG intensity as a function of the thickness of a Rb film on a Ag(110) surface. Such short wavelength oscillations would not be expected from an optical probe except where the signal is dominated by the surface or interface response: here they are attributed to Friedel-type screening oscillations extending from the surface into the metal. Figure 14(*b*) shows the normalised electron density from a

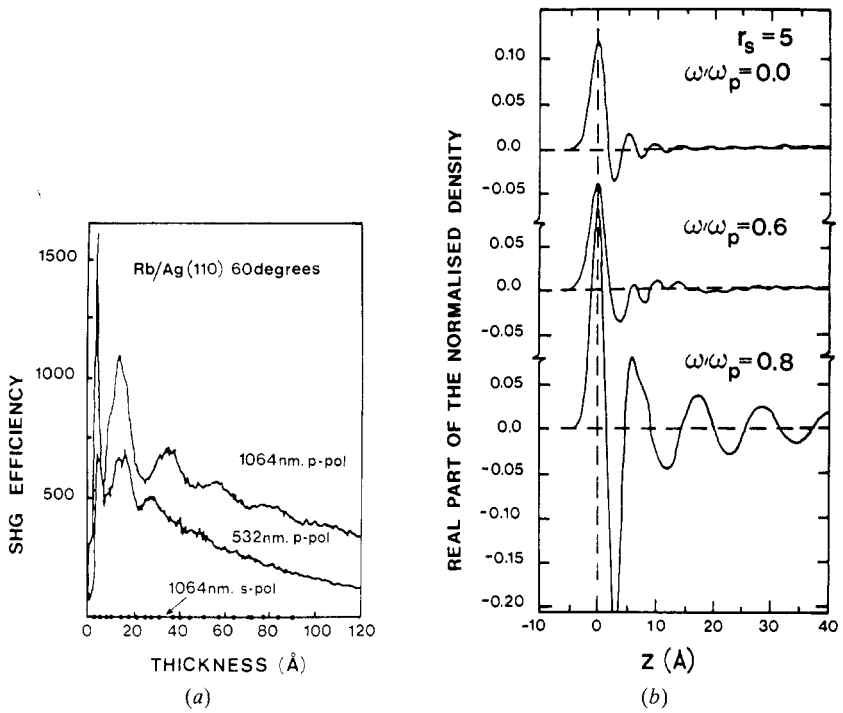

Figure 14. (*a*) SHG intensity as a function of Rb film thickness for two different wavelengths of p-polarised light. (*b*) Real part of the normalized density induced at a metal surface by a uniform electric field normal to the surface, for a screening radius, r_s, of 5 au (after Song *et al* 1988).

jellium calculation (Liebsch 1988, Liebsch and Schaich 1989) as a function of depth and excitation frequency. This direct imaging of the longitudinal screening field (note the lack of s-polarised signal in figure 14(*a*)) occurs because the oscillatory SHG intensity originates from the product of the longitudinal and transverse field strengths at the interface. The initial increase in the SHG intensity of a factor of 1600 at 1064 nm excitation wavelength, and of a factor of only 10 at 532 nm, remains to be explained (Song *et al* 1988). While the theoretical work is a most impressive start in this difficult field, it is clear that jellium calculations do not provide a complete explanation of surface SHG even from a simple metal like Al, as large band structure effects have been observed in the SH response from the Al(111) surface (Murphy *et al* 1989).

Frequency-dependent work on Ag(110) (Hicks *et al* 1988) has revealed a resonance maximum in the p-polarised SH response at $\simeq 3.9$ eV, just below the bulk plasma frequency where there is a minimum in the linear reflectivity (Wooten 1972). This is a bulk effect which appears even in simple hydrodynamic models of SH response (Corvi and Schaich 1986, Liebsch and Schaich 1989). Of greater potential importance is the frequency-dependent behaviour of the s-polarised SH response (figure 15), where these preliminary results are interpreted in terms of a resonance at ω associated with a transition between two surface states (Hicks *et al* 1990). This is an example of the spectroscopic dimension of surface and interface SHG which will become increasingly important as the technique matures.

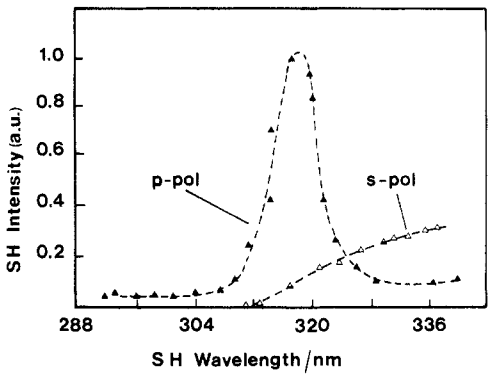

Figure 15. Variation of SHG with wavelength at an incident angle of 55° from Ag(110) at 298 K; filled triangles p-polarized light, open triangles s-polarized light (after Hicks *et al* 1990).

Studies of small molecule adsorption on metal surfaces have yielded a variety of interesting results. SHG studies of pyridine adsorption on Ag(110) at 110 K reveals, via the polarization dependence on the signal, a transition from a flat-lying phase at low coverage to a stand-up phase above 0.3 ML, in agreement with other work using conventional surface probes (Heskett *et al* 1988). SHG has been combined with work function studies of adsorbates on Re(0001) to show that electron-donating adsorbates such as H_2 and NH_3 decrease the work function and increase the SH signal, while electron withdrawing adsorbates such as O_2 and CO produce the opposite effect, in agreement with simple Drude ideas (Rosenzweig and Asscher 1988). This behaviour provides adsorbate-specificity of the SH response even in the absence of adsorbate electronic levels suitable for resonant SHG studies.

SHG has been used to measure the surface diffusion of CO on Ni(111) (Zhu *et al* 1988). In this elegant experiment the interference of two 1064 nm laser beams was used to prepare a monolayer grating of CO by desorption. A third beam of 532 nm was used for the SHG measurements. The specular SHG beam monitored the average CO coverage, while the time-dependence of the first order diffracted SHG beam provided a measure of the diffusion rate of the CO molecules, diffusion wiping out the diffraction grating with time (figure 16). The activation energy for diffusion obtained agreed well with other methods. This technique would appear to be particularly suited to measuring the dependence of diffusion on crystal azimuth.

A different type of small molecule study has been demonstrated by Shen's group (Hunt *et al* 1987). In a sum-frequency generation experiment, tunable IR radiation was mixed with visible radiation to obtain a visible sum-frequency signal which showed resonant enhancement at vibrational modes. This was used to obtain information about the vibrational spectra of adsorbed molecules on glass and water surfaces. Although not a UHV study, it is mentioned here as the technique has potential as an epioptic probe of vibrational, as opposed to electronic, structure.

Returning to semiconductor surfaces, two recent studies are of particular importance. In the first, surface SHG was observed from Sn adsorbed on GaAs(100) (Stehlin *et al* 1988). The substrate is noncentrosymmetric and has a bulk dipole response. Appropriate choice of polarizations and substrate orientation suppresses the bulk dipole response, while allowing many of the surface tensor components to be determined: surface SHG studies are thus not restricted to centrosymmetric systems (Stehlin *et al* 1988). In the second study, resonant SHG and sum-frequency generation has been applied

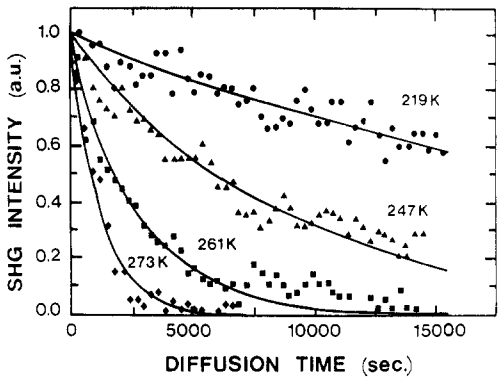

Figure 16. Normalized first order diffracted SHG, as a function of time, at various sample temperatures after laser desorption: ●, 219 K; ▲, 247 K; ■, 261 K; ◆, 273 K. The solid lines are fits to a one-dimensional diffusion equation (after Zhu *et al* 1988).

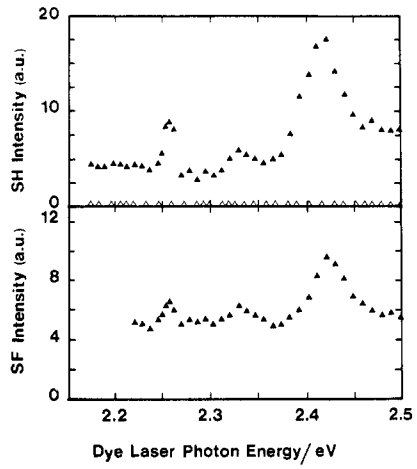

Figure 17. Resonant three-wave mixing, as a function of dye laser photon energy, from epitaxial CaF_2/Si(111). The open triangles refer to a native-oxide-covered Si(111) surface (after Heinz *et al* 1989).

to the buried CaF_2/Si(111) interface through 50 nm of CaF_2 (Heinz *et al* 1989). The importance of resonance effects in the full exploitation of surface and interface SHG has been stressed previously (McGilp and Yeh 1986, McGilp 1987a, b), and this work shows how resonant three-wave mixing may be used to determine an interface state band gap. Figure 17 shows that the dispersion of the sum-frequency signal matches the SH signal when plotted as a function of dye laser frequency. As the sum-frequency and SH signals occur at different frequencies, the resonance must occur at the dye laser frequency, allowing the bandgap at the buried interface to be measured (Heinz *et al* 1989). This is an excellent example of how an epioptic probe can provide unique information about the structure and properties of a buried interface between an insulator and a semiconductor.

5. Conclusion

This brief review of the optical spectroscopy of surfaces and interfaces has attempted to show the power and potential of epioptic techniques both in terms of the basic physics which may be investigated and the use of the techniques as diagnostic tools. The range of surface and interface systems accessible to each technique is not yet clear because many of the epioptic probes have not reached maturity. Some complementarity appears to exist between techniques exploiting linear and nonlinear susceptibilities, due to their different symmetries: RA works well for (100) and (110) surfaces, while SHG works best with (111) surfaces. Raman spectroscopy is a direct probe of the electric field at semiconductor interfaces via the Fröhlich effect, and strain in overlayers can be measured via changes in the deformation potential. Theoretical interest in the linear and nonlinear optical response of surfaces and interfaces may be expected to increase now that experimental results are appearing on a regular basis. These epioptic techniques are already being used at atmospheric pressure, and to probe solid–liquid interfaces.

The understanding and confidence gained from UHV studies will add great weight to such non-UHV studies in the future.

Acknowledgments

It is a pleasure to acknowledge useful discussions with Denis Weaire, Rodolfo Del Sole and Michele Cini. Thanks are due to D E Aspnes, E W Plummer and H-L Dai for communicating results prior to publication. This work has been supported by the EC ESPRIT Basic Research Action No 3177, 'EPIOPTIC'.

References

Acher O, Omnes F, Razeghi M and Drevillon B 1990 *Mater. Sci. Eng.* B **5** 223
Anderson R J M and Hamilton J C 1988 *Phys. Rev.* B **38** 8451
Andrieu S and Arnaud d'Avitaya F 1989 *Surf. Sci.* **219** 277
Aspnes D E 1985 *J. Vac. Sci. Technol.* B **3** 1498
Aspnes D E and Studna A A 1975 *Appl. Opt.* **14** 220
—— 1983 *Phys. Rev.* B **27** 985
—— 1985 *Phys. Rev. Lett.* **54** 1956
Aspnes D E, Harbison J P, Studna A A and Florez L T 1987 *Phys. Rev. Lett.* **59** 1687
—— 1988a *J. Vac. Sci. Technol.* A **6** 1327
Aspnes D E, Harbison J P, Studna A A, Florez L T and Kelly M K 1988b *Appl. Phys. Lett.* **52** 2046
—— 1988c *J. Vac. Sci. Technol.* B **6** 1127
Aspnes D E, Colas E, Studna A A, Bhat R, Koza M A and Keramidas V G 1988d *Phys. Rev. Lett.* **61** 2782
Aspnes D E, Bhat R, Colas E, Keramidas V G, Koza M A and Studna A A 1989 *J. Vac. Sci. Technol.* A **7** 711
Aspnes D E, Chang Y C, Studna A A, Florez L T, Farrell H H and Harbison J P 1990 *Phys. Rev. Lett.* **64** 192
Azzam R M A and Bashara N M 1977 *Ellipsometry and Polarized Light* (Amsterdam: North-Holland)
Berkovits V L, Makarenko I V, Minashvili T A and Safarov V I 1985 *Solid State Commun.* **56** 449
Berkovits V L, Ivantsov L F, Makarenko I V, Minashvili T A and Safarov V I 1987 *Solid State Commun.* **64** 767
Berkovits V L, Kiselev V A and Safarov V I 1989 *Surf. Sci.* **211/212** 489
Blanchet G B, Estrup P J and Stiles P J 1981 *Phys. Rev.* B **23** 3655
Bloembergen N, Chang R K, Jha S S and Lee C H 1968 *Phys. Rev.* **174** 813
Boyd G T, Shen Y R and Hansch T W 1986 *Opt. Lett.* **11** 97
Campion A 1987 *Vibrational Spectoscopy of Molecules on Surfaces* ed J T Yates Jr and T E Madey (New York: Plenum)
Chiaradia P, Chiarotti G, Ciccacci F, Memeo R, Nannarone S, Sassaroli P and Selci S 1980 *Surf. Sci.* **99** 70
Chiarotti G, Nannarone S, Pastore R and Chiaradia P 1971 *Phys. Rev.* B **4** 3398
Chiaradia P, Cricenti A, Selci S and Chiarotti G 1984 *Phys. Rev. Lett.* **52** 1145
Corvi M and Schaich W L 1986 *Phys. Rev.* B **33** 3688
Crean G M, Locatelli M and McGilp J (ed) 1990 *Acoustic, Thermal Wave and Optical Characterization of Materials (Eur. Mater. Res. Soc. Symp. Proc. 11)* (Amsterdam: North-Holland)
Damen T C, Porto S P S and Tell B 1966 *Phys. Rev.* **142** 570
Debe M K 1987 *Prog. Surf. Sci.* **24** 1
Del Sole R 1981 *Solid State Commun.* **37** 537
Del Sole R 1990 *Mater. Sci. Eng.* B **5** 177
Del Sole R and Seloni A 1984 *Phys. Rev.* B **30** 883
Feibelman P J 1982 *Prog. Surf. Sci.* **12** 287
Freeouf J L, Tsang J C, LeGoues F K and Iyer S S 1990 *Phys. Rev. Lett.* **64** 31
Gerhardt U and Rubloff G W 1969 *Appl. Opt.* **8** 305
Geurts J and Richter W 1987 *Springer Proceedings in Physics* vol 22 (Berlin: Springer) p 328
Gijzeman O L J and van Silfhout A (ed) 1983 *Special Volume in Commemoration of Gosse A. Bootsma; Surf. Sci.* **135**
Guidotti D, Driscoll T A and Gerritsen H J 1983 *Solid State Commun.* **46** 337
Guyot-Sionnest P, Chen W and Shen Y R 1986 *Phys. Rev.* B **33** 8254

Habraken F H M P, Gijzeman O L J and Bootsma G A 1980 *Surf. Sci.* **96** 482
Hallmark V M and Campion A 1986 *J. Chem. Phys.* **84** 2933
Heavens O S 1955 *Optical Properties of Thin Solid Films* (London: Butterworth)
Heinz T F 1982 *PhD Dissertation* University of California, Berkeley
Heinz T F, Loy M M T and Thompson W A 1985 *Phys. Rev. Lett.* **54** 63
Heinz T F, Himpsel F J, Palange E and Burstein E 1989 *Phys. Rev. Lett.* **63** 644
Heskett D, Urbach L E, Song K J, Plummer E W and Dai H-L 1988 *Surf. Sci.* **197** 225
Hicks J M, Urbach L E, Plummer E W and Dai H-L 1988 *Phys. Rev. Lett.* **61** 2588
—— 1990 *Proc. SPIE* to be published
Hollering R W J, Hoeven A J and Lenssinck J M 1990 *J. Vac. Sci. Technol.* A **8** 3194
Hopf F A and Stegeman G I 1986 *Applied Classical Electrodynamics* vols 1, 2 (New York: Wiley)
Huen T, Irani G B and Wooten F 1971 *Appl. Opt.* **10** 552
Hünermann M, Pletschen W, Resch U, Rettweiler U and Richter W 1987 *Surf. Sci.* **189/190** 322
Hunt J H, Guyot-Sionnest P and Shen Y R 1987 *Chem. Phys. Lett.* **133** 189
Kleint C and Merkel M 1989 *Surf. Sci.* **213** 657
Koort H J, Knorr K and Wiechert H 1987 *Surf. Sci.* **192** 187
Liebsch A 1988 *Phys. Rev. Lett.* **61** 1233
Liebsch A and Schaich W L 1989 *Phys. Rev.* B **40** 5401
Litwin J A, Sipe J E and van Driel H M 1985 *Phys. Rev.* B **31** 5543
Long D A 1977 *Raman Spectroscopy* (New York: McGraw-Hill)
Manghi F, Del Sole R, Molinari E and Selloni A 1989 *Surf. Sci.* **211/212** 518
McGilp J F 1989 *J. Phys.: Condens. Matter* **1** SB85
McGilp J F and Yeh Y 1986 *Solid State Commun.* **59** 91
McGilp J F 1987a *Semicond. Sci. Technol.* **2** 102
—— 1987b *J. Vac. Sci. Technol.* A **5** 1442
McIntyre J D E and Aspnes D E 1971 *Surf. Sci.* **24** 417
Mizrahi V and Sipe J E 1988 *J. Opt. Soc. Am.* B **5** 660
Murphy R, Yeganeh M, Song K J and Plummer E W 1989 *Phys. Rev. Lett.* **63** 318
Olmstead M A 1987 *Surf. Sci. Rep.* **6** 159
Olmstead M A and Amer N M 1984 *Phys. Rev. Lett.* **52** 1148
Pandey K C 1981 *Phys. Rev. Lett.* **47** 1913
—— 1982 *Phys. Rev. Lett.* **49** 223
Pinczuk A and Burstein E 1968 *Phys. Rev. Lett.* **21** 1073
Pletschen W, Esser N, Munder H, Zahn D, Geurts J and Richter W 1986 *Surf. Sci.* **178** 140
Richmond G L, Robinson J M and Shannon V L 1988 *Prog. Surf. Sci.* **28** 1
Rosenzweig Z and Asscher M 1988 *Surf. Sci.* **204** L732
Selci S, Chiaradia P, Ciccacci F, Cricenti A, Sparvieri N and Chiarotti G 1985 *Phys. Rev.* B **31** 4096
Selci S, Ciccacci F, Cricenti A, Felici A C, Goletti C and Chiaradia P 1987 *Solid State Commun.* **62** 833
Shen Y R 1984 *The Principles of Non-linear Optics* (New York: Wiley)
Shen Y R 1985 *J. Vac. Sci. Technol.* B **3** 1464
Sipe J E, Moss D J and van Driel H M 1987a *Phys. Rev.* B **35** 1129
Sipe J E, Mizrahi V and Stegeman G I 1987b *Phys. Rev.* B **35** 9091
Song K J, Heskett D, Dai H L, Liebsch A and Plummer E W 1988 *Phys. Rev. Lett.* **61** 1380
Stehlin T, Feller M, Guyot-Sionnest P and Shen Y R 1988 *Opt. Lett.* **13** 389
Straub D, Skibowski M and Himpsel F J 1985 *Phys. Rev.* B **32** 5237
Studna A A, Aspnes D E, Flores L T, Wilkens B J, Harbison J P and Ryan R E 1989 *J. Vac. Sci. Technol.* A **7** 3291
Tom H W K and Aumiller G D 1986 *Phys. Rev.* B **33** 8818
Tom H W K, Heinz T F and Shen Y R 1983 *Phys. Rev. Lett.* **51** 1983
Tom H W K, Mate C M, Zhu X D, Crowell J E, Heinz T F, Somorjai G A and Shen Y R 1984 *Phys. Rev. Lett.* **52** 348
Wierenga P E, van Silfhout A and Spaarnay M J 1979 *Surf. Sci.* **87** 43
Wierenga P E, van Silfhout A and Spaarnay M J 1980 *Surf. Sci.* **99** 59
Wooten F 1972 *Optical Properties of Solids* (New York: Academic)
Zahn D, Esser N, Pletschen W, Geurts J and Richter W 1986 *Surf. Sci.* **168** 823
Zandvliet H J W and van Silfhout A 1988 *Surf. Sci.* **195** 138
—— 1989 *Surf. Sci.* **211/212** 544
Zhu X D, Rasing T and Shen Y R 1988 *Phys. Rev. Lett.* **61** 2883